Rare-Earth Germanium Antimonides $RE_6Ge_{5-x}Sb_{11+x}$ (RE = La−Nd, Sm, Gd−Dy). II. Magnetic and Transport Properties

Laura Deakin, Robert Lam, and Arthur Mar*

Department of Chemistry, University of Alberta, Edmonton, Alberta, Canada T6G 2G2

Received August 17, 2000

Magnetic and transport properties have been measured for the series of ternary rare-earth germanium antimonides $RE_6Ge_{5-x}Sb_{11+x}$ (RE = La−Nd, Sm, Gd−Dy). All are metallic, with the members containing RE other than La displaying kinks in their resistivity vs temperature curves; the Tb and Dy members exhibit Kondo-like behavior with resistivity minima occurring at 10 and 150 K, respectively. For the compounds with RE = Ce, Pr, Nd, Sm, Gd, Tb, the magnetic susceptibility and electrical resistivity measurements reveal long-range antiferromagnetic ordering with $T_N \leq 22$ K. At 2 K, the Ce, Pr, and Nd members undergo metamagnetic transitions at critical fields between 1.0 and 4.0 T, while the Gd member displays spin-flop behavior with $H_{SF} = 1.85$ T and $H_C = 5.75$ T. The single-crystal magnetoresistance of the Gd member below T_N shows an orientationally dependent steplike behavior of resistivity as a function of field with changes in resistivity coinciding with the same critical fields observed in the magnetization measurements.

Introduction

The ternary rare-earth germanium antimonides $RE_6Ge_{5-x}Sb_{11+x}$ (RE = La−Nd, Sm, Gd−Dy)[1] possess a three-dimensional extended structure that can be decomposed in a "retrotheoretical" manner[2] into the electropositive RE and the electronegative metalloid (Ge, Sb) substructures. This decomposition of the structure into columns of face-sharing RE_6 trigonal prisms separated by "walls" of Ge and Sb atoms is useful from the chemical standpoint of isolating covalent interactions in order to rationalize the bonding in the complex metalloid network. In this contribution, we now turn our attention to the assemblies of RE atoms, which serve as the source of magnetic properties in these compounds. The orthorhombic structure of $RE_6Ge_{5-x}Sb_{11+x}$ (*Immm*, $Z = 2$), *with the metalloid substructure removed*, is shown in Figure 1. Examination of the interatomic distances between the RE atoms in the three members where single-crystal structures were determined (Table 1) shows that the *intra*column distances are shorter than the *inter*column distances by more than ∼1 Å, suggesting that these compounds may potentially display low-dimensional magnetism, with the nearest-neighbor interactions occurring within the columns. Although this type of arrangement of RE atoms has been observed in other compounds,[3] their magnetic and transport properties remain sparsely investigated. In view of the escalating interest that now surrounds ternary rare-earth antimonides in general, the extensive nature of the $RE_6Ge_{5-x}Sb_{11+x}$ series presents an ideal opportunity to explore the effect of RE substitution on the properties of an entire family of low-dimensional compounds. We report here the first studies on the magnetic and transport behavior of this series of compounds.

* To whom correspondence should be addressed. Telephone: (780) 492-5592. Fax: (780) 492-8231. E-mail: arthur.mar@ualberta.ca.

(1) Lam, R.; McDonald, R.; Mar, A. *Inorg. Chem.* **2001**, *40*, 952.
(2) Papoian, G.; Hoffmann, R. *J. Solid State Chem.* **1998**, *139*, 8.
(3) Sologub, O.; Vybornov, M.; Rogl, P.; Hiebl, K.; Cordier, G.; Woll, P. *J. Solid State Chem.* **1996**, *122*, 266.

Experimental Section

Synthesis. All compounds were prepared as described previously.[1] All transport measurements were made on single crystals whose composition was verified by EDX analyses on a scanning electron microscope. Initial magnetic studies were made on a sample totaling ∼10 mg of individually selected single crystals of $Gd_6Ge_{4.3(1)}Sb_{11.7(1)}$, as verified by EDX analyses. Corresponding measurements were made on a sample of $Gd_6Ge_{4.3(1)}Sb_{11.7(1)}$ from the bulk product and gave identical results. For all other compounds except $Dy_6Ge_{5-x}Sb_{11+x}$, magnetic measurements were made on samples from the bulk product, which were checked for purity by X-ray powder diffraction on a Guinier camera. Magnetic measurements were not carried out on $Dy_6Ge_{5-x}Sb_{11+x}$, which could only be produced in ∼25% purity.

Transport Measurements. Electrical resistivities of single crystals (needles typically 0.02−0.05 mm wide and 0.5−2.0 mm long) were measured with the current parallel to the needle axis (crystallographic *a* axis) by standard four-probe techniques on a Quantum Design PPMS system using an ac transport controller (Model 7100). Magnetoresistance measurements were made with the current parallel to the needle axis and with the crystal oriented parallel and perpendicular to the applied field using a horizontal rotator probe. A current of 0.05 mA and a frequency of 16 Hz were used.

Magnetic Measurements. Magnetic data were obtained on powders placed in gelcap sample holders with a Quantum Design 9T-PPMS dc magnetometer/ac susceptometer between 2 and 300 K and in applied fields up to 9 T. ac magnetic susceptibility measurements were made with a driving amplitude of 1 Oe and frequencies between 10 and 2000 Hz. Additional isothermal magnetization experiments were carried out on single crystals of $Gd_6Ge_{4.3(1)}Sb_{11.7(1)}$, all aligned in the same direction (needle axis parallel to applied field) and attached with Kapton tape on the gelcap holder. All susceptibility values were corrected for contributions from the holder diamagnetism and the underlying sample diamagnetism using the following values (emu/mol): RE, -20×10^{-6}; Ge, -7×10^{-6}; Sb, -15×10^{-6}.

Results and Discussion

Transport Properties. All $RE_6Ge_{5-x}Sb_{11+x}$ members are metallic, as indicated by their resistivity curves (Figure 2). For RE = Ce−Nd, Sm, Gd, the change in slope of the resistivity at

10.1021/ic0014078 CCC: $20.00
Published on Web 01/30/2001

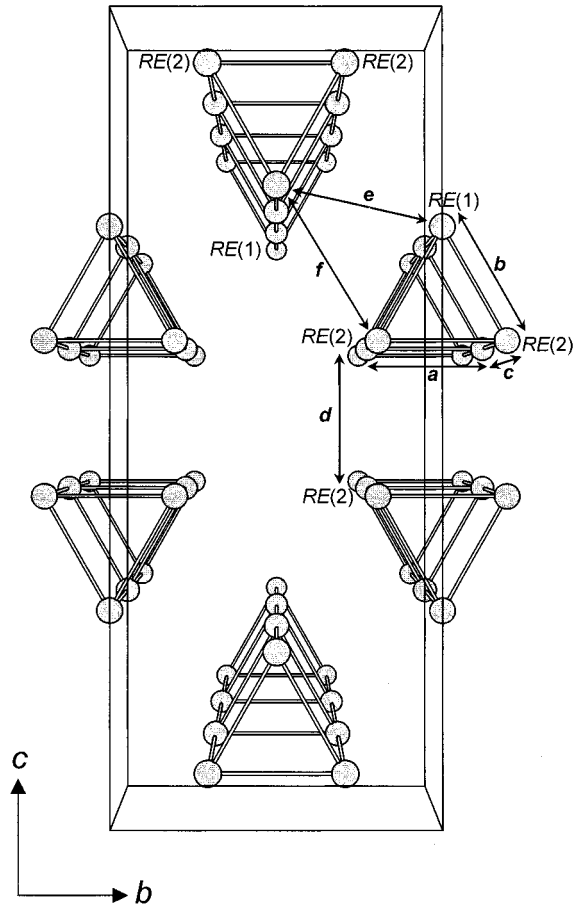

Figure 1. Structure of $RE_6Ge_{5-x}Sb_{11+x}$ viewed down the *a* axis, with the Ge and Sb atoms omitted. The *RE* atoms are arranged in trigonal-prismatic columns. Distances labeled ***a*−*f*** are listed in Table 1 for the members whose crystal structures have been determined.

Table 1. Interatomic Rare-Earth Distances (Å)[a] in $RE_6Ge_{5-x}Sb_{11+x}$ (*RE* = La, Nd, Gd)

RE−*RE* dist[b]	$La_6Ge_{2.8(1)}$-$Sb_{13.2(1)}$	$Nd_6Ge_{3.6(1)}$-$Sb_{12.4(1)}$	$Gd_6Ge_{4.3(1)}$-$Sb_{11.7(1)}$
	Intracolumn		
a	4.218	4.112	4.020
b	4.306	4.226	4.161
c	4.303	4.231	4.151
	Intercolumn		
d	5.120	5.033	5.025
e	5.907	5.785	5.677
f	6.113	5.975	5.868

[a] All esds are less than 0.001 Å. [b] Refer to Figure 1 for labeling of distances.

low temperatures (insets of Figure 2a,b) is attributed to the loss in spin-disorder scattering upon establishment of long-range magnetic ordering. The most dramatic effects are observed in the Ce member, whose resistivity becomes temperature independent below 20 K (but does not reach a minimum) and then rapidly decreases below 5 K (Figure 2a). The transition temperatures at which these slope changes occur in the resistivity curves correspond to the Néel ordering temperatures T_N determined by magnetic susceptibility studies, discussed later. These members all exhibit residual resistivity ratios ($\rho_{300\ K}/\rho_{2\ K}$) close to 2.0 (Table 2), consistent with the partial disorder of Ge and Sb found in the crystal structure of these phases.

For *RE* = Tb, Dy, the resistivity does not decrease continuously with decreasing temperature but, rather, shows strikingly

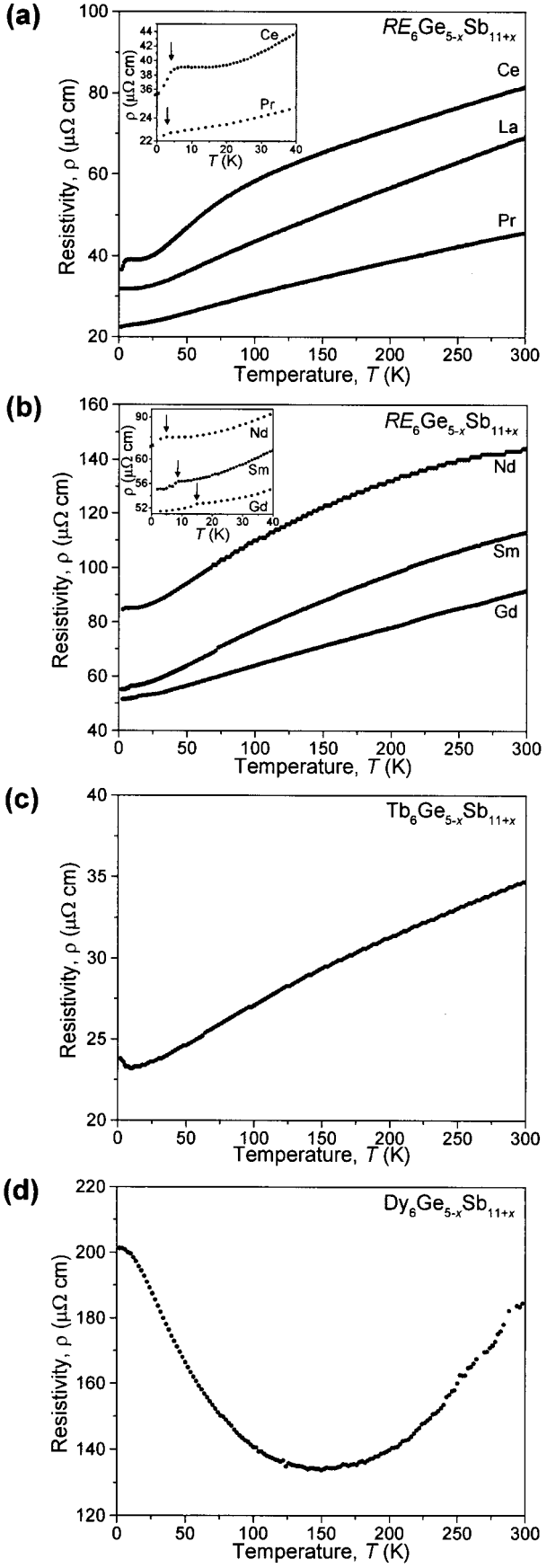

Figure 2. Electrical resistivity of single crystals of $RE_6Ge_{5-x}Sb_{11+x}$ measured along the *a* axis between 2 and 300 K: (a) *RE* = La, Ce, Pr; (b) *RE* = Nd, Sm, Gd; (c) *RE* = Tb; (d) *RE* = Dy. Insets of (a) and (b) show low-temperature behavior, the arrows indicating changes in slope arising from magnetic ordering.

Table 2. Summary of Resistivity and Magnetism Data for $RE_6Ge_{5-x}Sb_{11+x}$

compd	$\rho_{300\ K}/\rho_{2\ K}$	μ_{eff}(300 K) (μ_B/RE^{3+})	μ_{RS} (μ_B/RE^{3+})	θ (K)	T_N (K)	H_{SF}(2 K) (T)	H_C(2 K) (T)
$La_6Ge_{5-x}Sb_{11+x}$	2.18						
$Ce_6Ge_{5-x}Sb_{11+x}$	2.23	2.58	2.54	−27	4.0		1.0
$Pr_6Ge_{5-x}Sb_{11+x}$	2.03	3.54	3.58	−8	2.7		1.5
$Nd_6Ge_{5-x}Sb_{11+x}$	1.70	3.94	3.62	−53	4.2		4.0
$Sm_6Ge_{5-x}Sb_{11+x}$	2.05	1.2	0.85		8.3		
$Gd_6Ge_{5-x}Sb_{11+x}$	1.77	7.08	7.94	−47	12.5	1.85	5.75
$Tb_6Ge_{5-x}Sb_{11+x}$	1.46	8.53	9.72	−10	22		>7
$Dy_6Ge_{5-x}Sb_{11+x}$	0.92						

different behavior from the other members, attaining pronounced minima in their curves at 10 and 150 K, respectively (Figure 2c,d). Not only does the resistivity minimum for the Dy member occur at much higher temperatures than for the Tb member but the resistivity is also greater at low temperatures than at room temperature ($\rho_{2\ K} > \rho_{300\ K}$) and it becomes temperature independent below 10 K, reaching a constant value of ~200 $\mu\Omega$ cm. These two resistivity minima are reminiscent of Kondo-like behavior, in which interactions between the localized f electrons and the conduction electrons lead to a compensation of the *RE* moments.[4] Such resistivity minima have also been observed in compounds that additionally display colossal magnetoresistance.[5] The absence of a further decrease in resistivity at very low temperatures suggests that long-range magnetic ordering does not occur in this temperature range. The formation of magnetic vs nonmagnetic ground states resulting from Ruderman−Kittel−Kasuya−Yosida (RKKY) or Kondo interactions of *RE* ions with other spin sites or with the conduction electrons, respectively, remains a topic that receives much attention.[6] For compounds containing rare-earth elements other than Ce and Yb, however, the energy difference between the f electrons and the Fermi level inhibits the antiferromagnetic Kondo-type interactions between the rare-earth and conduction electrons.[4] The observation of resistivity minima for several late-rare-earth intermetallic alloys has led to the postulation that short-range magnetic interactions, present before long-range order is established, may be contributing to this resistivity behavior.[7] In the case of $RE_6Ge_{5-x}Sb_{11+x}$, the short-range magnetic interactions would occur within the 1D arrangements of *RE* trigonal-prismatic columns.

Magnetic and Magnetoresistive Behavior. Table 2 summarizes the magnetic properties observed in the $RE_6Ge_{5-x}Sb_{11+x}$ series of compounds, which range from the nonmagnetic ($La_6Ge_{5-x}Sb_{11+x}$) to those that are magnetically ordered antiferromagnets ($RE_6Ge_{5-x}Sb_{11+x}$ with *RE* = Ce−Nd, Sm, Gd, Tb). The magnetic behavior for the Dy member could not be determined, owing to unsatisfactory purity of the bulk powder.

$Ce_6Ge_{5-x}Sb_{11+x}$. As the temperature is lowered, the effective moment decreases slightly to reach a minimum at ~45 K (θ = −27 K; 150 < *T* < 300 K), increases to reach a maximum at 5 K, and then rapidly decreases upon approaching 2 K (Figure 3a). Isothermal magnetization measurements made at 2 K revealed a metamagnetic transition at H_C = 1.0 T, manifested as a sudden increase in magnetization, which saturates at M_{sat} = 1.35 μ_B/Ce (Figure 3b). The temperature dependence of the χ'_{ac} (linear in-phase) magnetic susceptibility indicates that long-range antiferromagnetic order is established at T_N = 4.0 K, where the maximum in $d\chi'/dT$ occurs (Figure 3c). The value of T_N determined from the magnetic data here coincides with the change in slope in the resistivity data (Figure 2a).

While there may be small contributions from other magnetic phases, as seen by the weak shoulder in χ'_{ac} at ~10 K, they must be minimal, as no impurity phases were observed by powder X-ray diffraction. The potential binary impurity $CeSb_2$ can be ruled out, since it is known to undergo ferromagnetic ordering at T_C = 15 K.[8] The maximum in μ_{eff} is then attributed to the occurrence of a spontaneous moment generated from short-range 1D interactions within the trigonal-prismatic columns. The spontaneous moment may be arising either from a ferrimagnetic (↑↑↓) spin arrangement within the *RE* triangles or from a canted spin structure between triangles of a column. The ferrimagnetic triangular spin structure could be stabilized by the inequivalent bond distances between the *RE* atoms (d(Ce(1)−Ce(2)) (× 2) ≠ d(Ce(2)−Ce(2)) (Figure 1), forming an isosceles triangle and avoiding a frustrated spin geometry. Both scenarios lead to the formation of a spontaneous moment from 1D interactions along the trigonal-prismatic columns, followed by long-range magnetic interactions leading to antiferromagnetic ordering at T_N. As noted earlier, the intracolumn *RE*−*RE* distances are markedly shorter than the intercolumn *RE*−*RE* distances. The observation of a spontaneous moment in $Ce_6Ge_{5-x}Sb_{11+x}$ is therefore a manifestation of the structural and magnetic low-dimensionality of these compounds.

$Pr_6Ge_{5-x}Sb_{11+x}$ and $Nd_6Ge_{5-x}Sb_{11+x}$. Both compounds display similar magnetic behavior (Figure 3d), with the effective moment decreasing as the temperature is lowered ($Pr_6Ge_{5-x}Sb_{11+x}$, θ = −8 K, μ_{eff}(300 K) = 3.54 μ_B/Pr; $Nd_6Ge_{5-x}Sb_{11+x}$, θ = −53 K, μ_{eff}(300 K) = 3.94 μ_B/Nd). The μ_{eff} value for $Pr_6Ge_{5-x}Sb_{11+x}$ at 300 K is very close to that expected according to Russell−Saunders coupling (Table 2). The slow increase in effective moment as the temperature is raised for $Nd_6Ge_{5-x}Sb_{11+x}$ is likely due to a temperature-independent paramagnetic contribution, which results in the large magnitude of θ and a slightly higher than expected μ_{eff} value. $Pr_6Ge_{5-x}Sb_{11+x}$ and $Nd_6Ge_{5-x}Sb_{11+x}$ show long-range antiferromagnetic ordering at T_N = 2.7 and 4.2 K, respectively (Figure 3c), and they display neither a maximum in the χ''_{ac} magnetic susceptibility nor a frequency dependence of the χ'_{ac} signal. As with the Ce member, $Pr_6Ge_{5-x}Sb_{11+x}$ and $Nd_6Ge_{5-x}Sb_{11+x}$ also undergo a metamagnetic transition at 2 K, at H_C = 1.5 and 4.0 T, respectively (Figure 3b).

The trend of decreasing effective moment with decreasing temperature is consistent with the presence of antiferromagnetic

(4) Hewson, A. C. *The Kondo Problem to Heavy Fermions*; Cambridge University Press: Cambridge, U.K., 1997.
(5) (a) Shimakawa, Y.; Kubo, Y.; Manako, T. *Nature* **1996**, *379*, 53. (b) Subramanian, M. A.; Toby, B. H.; Ramirez, A. P.; Marshall, W. J.; Sleight, A. W.; Kwei, G. H. *Science* **1996**, *273*, 81.
(6) (a) Spałek, J.; Doradziński, F. In *Magnetism and Electronic Correlations in Local-Moment Systems*: *Rare-Earth Elements and Compounds*; Donath, M., Dowben, P. A., Nolting, W., Eds.; World Scientific: Singapore, 1998; pp 387−405. (b) Bernhard, B. H.; Lacroix, C.; Iglesias, J. R.; Coqblin, B. *Phys. Rev. B* **2000**, *61*, 441. (c) Moeller, G.; Dobrosavljević, V.; Ruckenstein, A. E. *Phys. Rev. B* **1999**, *59*, 6846.
(7) Mallik, R.; Sampathkumaran, E. V. *Phys. Rev. B* **1998**, *58*, 9178 and references therein.
(8) Canfield, P. C.; Thompson, J. D.; Fisk, Z. *J. Appl. Phys.* **1991**, *70*, 5992.

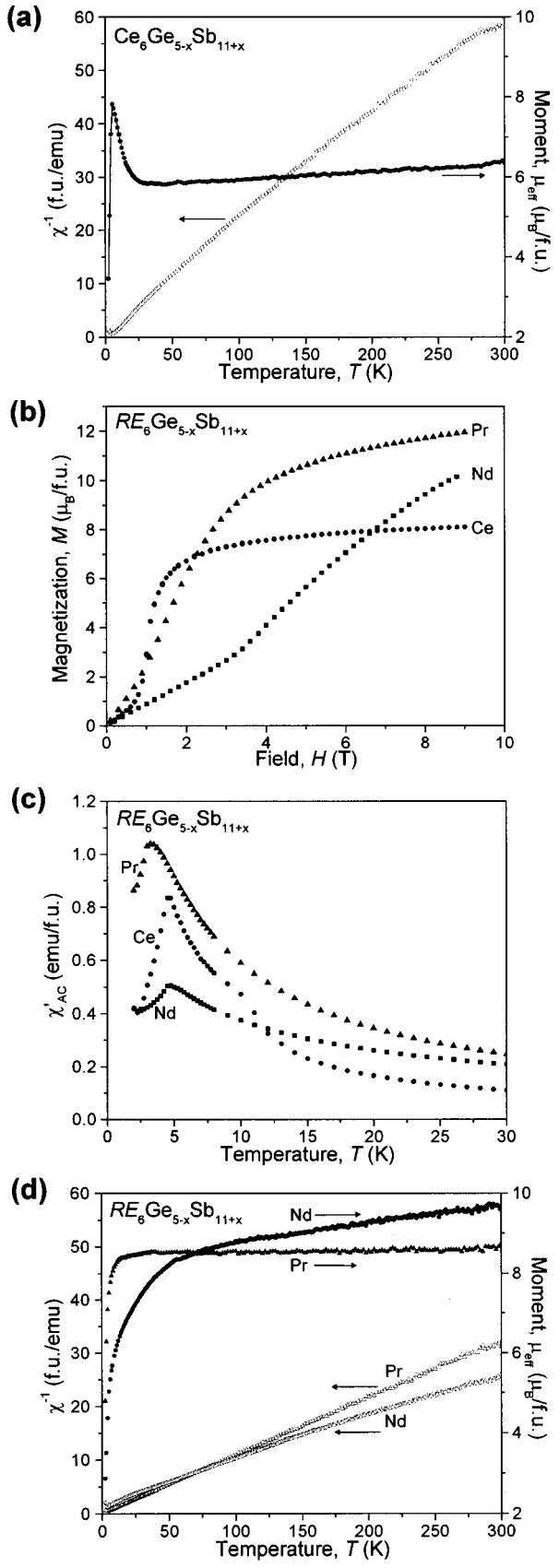

Figure 3. Magnetic data for $RE_6Ge_{5-x}Sb_{11+x}$ (RE = Ce, Pr, Nd): (a) effective moment and inverse molar magnetic susceptibility for RE = Ce in an applied field of 0.1 T (the line for the moment plot is included only to guide the eye); (b) isothermal magnetization at T = 2 K; (c) χ'_{ac} magnetic susceptibility (1 Oe, ν = 1000 Hz); (d) effective moment and inverse molar magnetic susceptibility for RE = Pr, Nd in an applied field of 0.1 T.

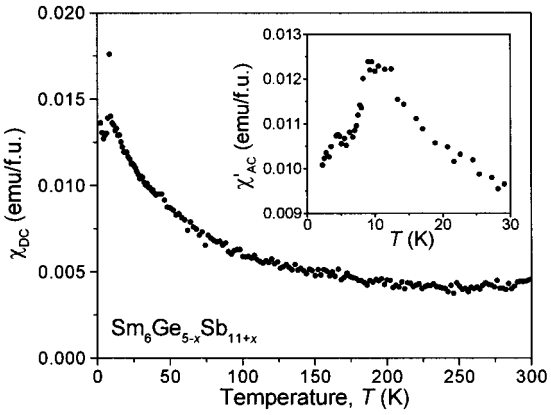

Figure 4. Molar magnetic susceptibility χ_{dc} of $Sm_6Ge_{5-x}Sb_{11+x}$ in an applied field of 0.5 T. Inset: χ'_{ac} magnetic susceptibility (1 Oe, ν = 1000 Hz).

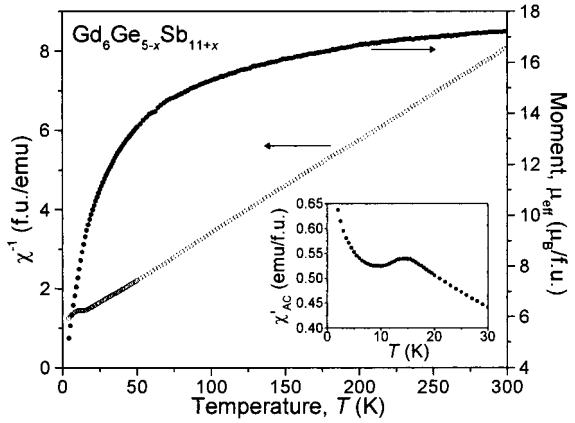

Figure 5. Effective moment and inverse molar magnetic susceptibility of $Gd_6Ge_{5-x}Sb_{11+x}$ in an applied field of 0.1 T. Inset: χ'_{ac} magnetic susceptibility (1 Oe, ν = 1000 Hz).

interactions between *RE* atoms. This spin arrangement could result from a ferromagnetic alignment within triangles and antiferromagnetic alignment between triangles within a column, leading to an antiferromagnetically ordered ground state below T_N. The magnetism of $RE_6Ge_{5-x}Sb_{11+x}$ for RE = Pr, Nd is unlike that for RE = Ce in that the former do not display evidence of a spontaneous moment from low-dimensional short-range magnetic interactions.

$Sm_6Ge_{5-x}Sb_{11+x}$. The variable-temperature susceptibility (Figure 4) shows a maximum at ~9 K and van Vleck paramagnetism at higher temperatures (μ_{eff}(300 K) = 1.2 μ_B/Sm). The χ'_{ac} magnetic susceptibility behavior (inset of Figure 4) is consistent with long-range antiferromagnetic magnetic ordering at T_N = 8.3 K; no χ''_{ac} maximum was observed. Below T_N, the isothermal magnetization does not display metamagnetic behavior, as it increases linearly with field up to 9 T. Since the high-temperature regime of the susceptibility curve does not follow the Curie−Weiss law, the temperature dependence of effective moment cannot be interpreted in a simple way. However, it is presumed that antiferromagnetic interactions between triangles of *RE* atoms within the columns, similar to the type postulated for RE = Pr, Nd, are also operative here.

$Gd_6Ge_{5-x}Sb_{11+x}$. The temperature dependence of the effective moment (μ_{eff}(300 K) = 7.08 μ_B/Gd; θ = −47 K; 150 < T < 300 K) and the χ'_{ac} magnetic susceptibility maximum indicate that the Gd atoms interact antiferromagnetically, with long-range order being established at T_N = 12.5 K (Figure 5). The field dependence of the magnetization at 2 K, however, is

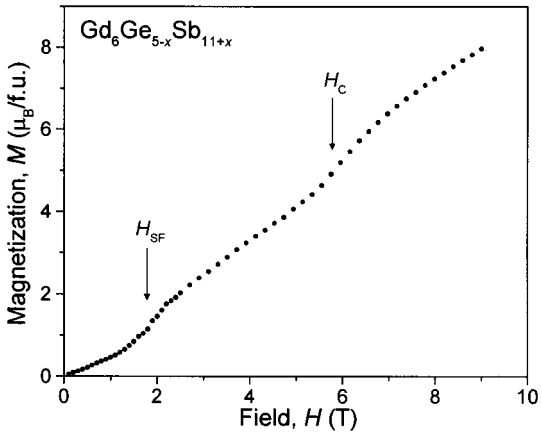

Figure 6. Magnetization of aligned $Gd_6Ge_{5-x}Sb_{11+x}$ single crystals at $T = 2$ K with $H \parallel a$. The critical fields occur at $H_{SF} = 1.85$ and $H_C = 5.75$ T.

unique to this *RE* member. There is a change in slope in the *M* vs *H* curve for aligned single crystals of $Gd_6Ge_{5-x}Sb_{11+x}$ at two critical fields (Figure 6). Both of these kinks are absent in the corresponding curve for a powder sample of $Gd_6Ge_{5-x}Sb_{11+x}$. The magnetization does not saturate at fields up to 9 T. These effects are interpreted to result from spin-flop behavior: at the first critical field ($H_{SF} = 1.85$ T), the spins flop into an arrangement perpendicular to the applied field, and at the second critical field ($H_C = 5.75$ T), the spins are realigned parallel to the applied field.[9] The formation of an intermediate spin-flopped phase has been observed in other compounds containing Gd^{3+} ions,[10] whose $^8S_{7/2}$ ground state leads to the low magnetocrystalline anisotropy necessary for spin flopping to occur. Thus, in the $RE_6Ge_{5-x}Sb_{11+x}$ series, spin flopping is seen only for the Gd member, while metamagnetism is seen for the members containing Ce, Pr, and Nd, whose larger magnetocrystalline anisotropy permits only a direct transition from an antiferromagnetic to a ferromagnetic spin alignment without an intermediate spin-flopped phase. Although the orientation dependence of the magnetization of a single crystal of $Gd_6Ge_{5-x}Sb_{11+x}$ could not be examined, owing to instrument constraints, it could be inferred from magnetoresistance measurements.

Figure 7 shows plots of the resistivity vs field for a single crystal of $Gd_6Ge_{5-x}Sb_{11+x}$ at various temperatures below T_N with the applied field oriented parallel or perpendicular to the crystal needle axis (crystallographic *a* axis). Steps are observed in these curves ($H \parallel a$) which disappear as the temperature approaches T_N. At 2 K and $H \parallel a$, critical fields are revealed at similar values determined from the magnetization study above. The resistivity increases steeply with increasing field to $H_{SF} = 1.56$ T, then increases more gradually, and finally decreases sharply at $H_C = 5.53$ T. At 2 K and $H \perp a$, the slope is also positive with only a small change in slope at ~1.5 T, which may be a result from a slight crystal tilting in the mounting procedure. These features are consistent with spin-flop behavior and result from changes in the magnetization and effective carrier number.[11] At low fields $H < H_{SF}$, the magnetoresistance ($[\rho(H) - \rho(0)]/\rho(0)$) is positive and the resistivity is proportional to H^2 when $H \parallel a$, as expected for an antiferromagnet whose

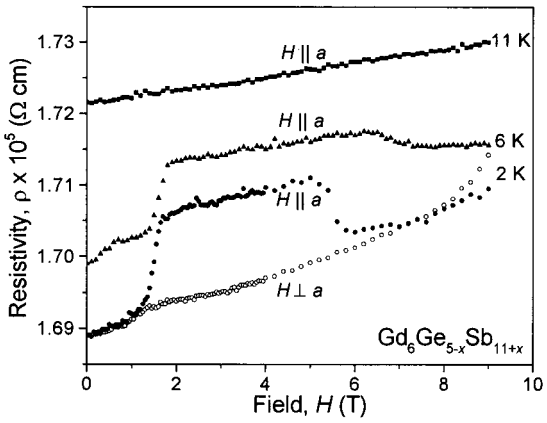

Figure 7. Field and orientation dependence of electrical resistivity of a single crystal of $Gd_6Ge_{5-x}Sb_{11+x}$ at 2 K ($H \perp a$ and $H \parallel a$), 6 K ($H \parallel a$), and 11 K ($H \parallel a$).

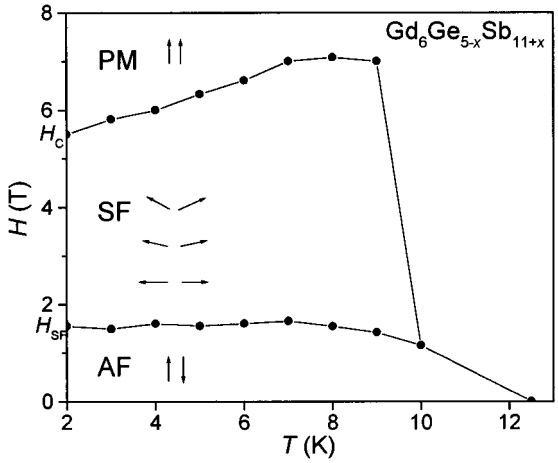

Figure 8. Magnetic phase diagram of $Gd_6Ge_{5-x}Sb_{11+x}$ determined from magnetoresistance measurements with $H \parallel a$. Definitions: AF, antiferromagnetic; SF, spin-flop; PM, paramagnetic.

magnetization axis is parallel to the applied field. In the region $H_{SF} < H < H_C$, the magnetoresistance is expected to become zero for a perpendicular orientation of the magnetization axis, but the observation of a continuing rise in resistivity with increasing field suggests that there is a field-induced change in effective carrier number. At high fields $H > H_C$ when $H \parallel a$, the resistivity decreases as the sample converts to a paramagnetic state.

The observation of changes in magnetization only when $H \parallel a$ (Figure 6) at the critical fields H_{SF} and H_C, confirmed by the single-crystal magnetoresistance measurements (Figure 7), places the magnetization axis in the antiferromagnetic phase of $Gd_6Ge_{5-x}Sb_{11+x}$ parallel to the trigonal-prismatic columns of *RE* atoms. From the critical fields deduced by magnetoresistance measurements, a magnetic phase diagram showing the occurrence of the antiferromagnetic and spin-flop phases can be determined (Figure 8). Similar steplike changes in resistivity as a function of field have been reported for $CeSb_2$[12] and Gd_2PdSi_3[13] and have been attributed to metamagnetic transitions.

$Tb_6Ge_{5-x}Sb_{11+x}$. The effective moment decreases gradually as the temperature is lowered ($\theta = -10$ K; $150 < T < 300$ K) and then decreases rapidly below ~50 K (Figure 9a). Similar

(9) DeJongh, L. J.; Miedema, A. R. *Experiments on Simple Magnetic Model Systems*; Taylor & Francis: London, 1974.
(10) (a) Hulliger, F. In *Handbook on the Physics and Chemistry of Rare Earths*; Gschneidner, K. A., Jr., Eyring, L., Eds.; North-Holland: Amsterdam, 1979; pp 153−236, and references therein. (b) Cashion, J. D.; Cooke, A. H.; Thorp, T. L.; Wells, M. R. *Proc. R. Soc. London, Ser. A* **1970**, *318*, 473.
(11) Yamada, H.; Takada, S. *J. Phys. Soc. Jpn.* **1973**, *34*, 51.
(12) Bud'ko, S. L.; Canfield, P. C.; Mielke, C. H.; Lacerda, A. H. *Phys. Rev. B* **1998**, *57*, 13624.
(13) Saha, S. R.; Sugawara, H.; Matsuda, T. D.; Sato, H.; Mallik, R.; Sampathkumaran, E. V. *Phys. Rev. B* **1999**, *60*, 12162.

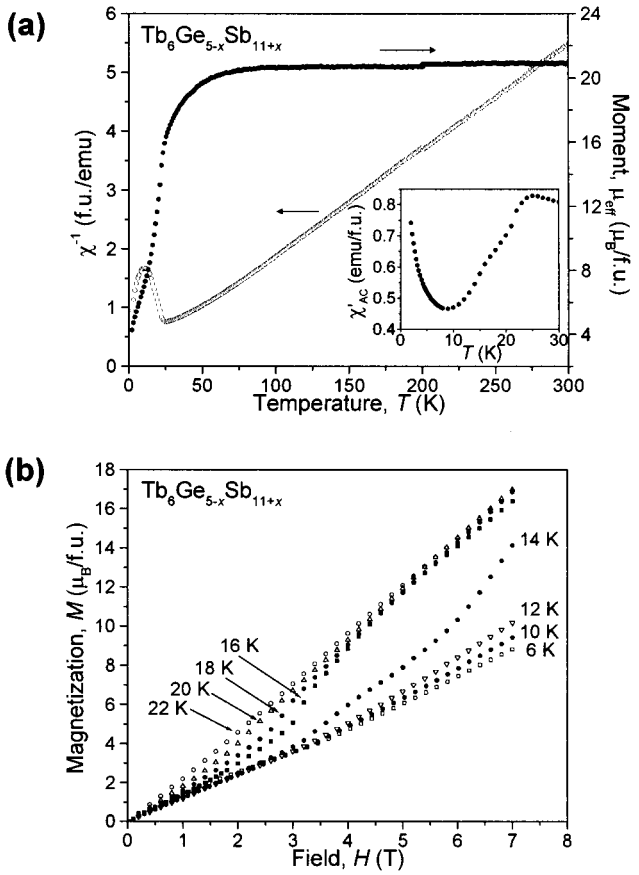

Figure 9. (a) Effective moment and inverse molar magnetic susceptibility of $Tb_6Ge_{5-x}Sb_{11+x}$ in an applied field of 0.1 T. Inset: χ'_{ac} magnetic susceptibility (1 Oe, $\nu = 1000$ Hz). (b) Isothermal magnetization of $Tb_6Ge_{5-x}Sb_{11+x}$ in fields up to 7.0 T between 6 and 22 K.

to the previous cases (*RE* = Ce, Pr, Nd, Sm, Gd), antiferromagnetic interactions are proposed for $Tb_6Ge_{5-x}Sb_{11+x}$ as isothermal magnetization measurements made at $T < 22$ K show a metamagnetic transition (Figure 9b). For this rare-earth member, T_N is 22 K, as determined from the maximum in $d\chi'/dT$ (inset of Figure 9a). The minimum observed in the χ_{dc} and χ'_{ac} magnetic susceptibilities is not seen for any other of the rare-earth members and occurs at the temperature where a minimum was observed in the resistivity (Figure 2c). This member is the only one in the $RE_6Ge_{5-x}Sb_{11+x}$ series that does not display a decrease in resistivity at T_N. The increase in χ'_{ac} and resistivity at $T < 8$ K may be due to the presence of another magnetic phase at very low temperatures—perhaps a glassy state.

Conclusion

The Ce, Pr, Nd, Sm, Gd, and Tb members of the $RE_6Ge_{5-x}Sb_{11+x}$ series undergo long-range antiferromagnetic ordering with $T_N \leq 22$ K. The three early-rare-earth compounds undergo a metamagnetic transition between 1 and 4 T; such a field-induced transition is not observed for the Sm member below T_N. Although the Ce member is an antiferromagnet below T_N, this compound displays unique magnetic properties in which a spontaneous moment arises from short-range 1D magnetic interactions along the trigonal-prismatic columns of *RE* atoms. From the single-crystal magnetization and magnetoresistance measurements that show two critical fields at temperatures below T_N, it is suggested that the Gd member goes through a field-induced spin-flop phase. The Tb member also possesses an antiferromagnetic ground state; however, the metamagnetic transition occurs at very large critical fields ($H_C > 7$ T at 2 K). Anisotropic magnetic susceptibility and magnetoresistance measurements may help clarify the nature of the magnetic structure in all these compounds, but a full neutron diffraction study is ultimately required. The resistivity curves for the Tb and Dy members have greatly different properties from the earlier *RE* members, showing pronounced minima. Since the unit cell contracts upon substitution with later *RE* elements, decreasing *RE*−*RE* separations, it is evident that other factors, such as the hybridization of the f electrons with the conduction electrons, have an important influence on the magnetic and transport properties. It is hoped that a comparison of results from band structure calculations for each rare-earth member may provide insight into the difference in magnetic and transport properties observed.

Acknowledgment. Financial support from the Natural Sciences and Engineering Research Council of Canada, the Province of Alberta, and the University of Alberta is gratefully acknowledged. We thank Christina Barker for assistance with the EDX analyses.

IC0014078